

Revisiting The Phase Diagram of Au – Cu Alloy at Nanoscales

F. Monji¹, M. A. Jabbareh^{2*}

¹Department of Mechanical Engineering, York University, Toronto, ON M3J 1P3, Canada.

²Department of Materials and Polymer Engineering, Faculty of Engineering, Hakim Sabzevari University, Sabzevar, Iran.
E-mail: ¹fmonji@yorku.ca, ²m.jabbareh@hsu.ac.ir

Received 27 September 2021, Revised 14 December 2021, Accepted 24 February 2022

Abstract

Au – Cu nanoparticles are widely used as catalysts in different chemical reactions. Since knowing the phase diagram of nano-alloys is crucial for effective design of nano-catalysts, there have been many efforts to predict the size effect on the phase diagram of the Au – Cu system. However, reported results are inconsistent and sometimes contradictory. In this work, a CALPHAD type thermodynamic model was applied to recalculate the phase diagram of Au – Cu binary alloy nanoparticles at different sizes. The results show that decreasing particle size decreases liquidus and solidus temperatures as well as the congruent melting point. It was also found that by reduction of the particle size, the composition of the congruent alloy shifts towards the Au – rich side of the phase diagram.

Keywords: *Size effect; alloy nanoparticle; Au – Cu alloy; phase diagram; CALPHAD method.*

1. Introduction

Gold - Copper (Au-Cu) alloy nanoparticles have attracted considerable interest in nanoscience and nanotechnology, especially as catalysis. They are widely used in the oxidation of carbon monoxide [1], reduction of carbon dioxide [2], selective oxidation of alcohols [3], and other chemical reactions [4,5]. It has been shown that the catalytic efficiency of nanoparticles directly depends on their melting temperatures [6]. Therefore, to achieve optimum performance, the knowledge of nanoscale phase diagram of desired system is essential for tuning the properties and optimal design of nano-catalysts. Since the calorimetric measurements are very difficult to apply to nanoparticles, theoretical methods are generally used for predicting phase diagrams at nanoscales [7,8].

Due to its importance, there have been several attempts to calculate the size dependent phase diagram of Au – Cu nano-alloy in recent years. Using their thermodynamic model, Vallee et al. [9] calculated the phase diagram of spherical Au – Cu nanoparticles with 106 atoms (~ 30 nm in diameter). They showed that compared to the bulk, at nanoscales solidus and liquidus temperatures drop to lower temperatures. According to their results, the congruent melting point had a shift to the Au – rich side of the Au – Cu phase diagram when the particle size dropped to the nanoscale. Guisbiers et al. [10] adopted a nano-thermodynamic model and calculated the phase diagram of different polyhedral Au – Cu nanoparticles at sizes of 4 and 10 nm. Regardless of the geometry of the nanoparticles, similar to Vallee et al., their results demonstrated a decrease in solidus and liquidus temperatures by decreasing particle size. However, in contrast to the results reported by Vallee et al., calculations by Guisbiers et al. showed a considerable shift in the congruent melting point towards Cu – rich side of the phase diagram. Based on the size dependent cohesive energy model, Cui et al. [11] developed a nano-thermodynamic model and investigated the effects of size,

shape, and segregation on the phase diagram of polyhedral and spherical Au-Cu nanoparticles at sizes of 4 and 10 nm. For spherical nanoparticles with a diameter of 4 nm, they reported a decrease of 400, 340, and 340 K in melting temperature of Au, Cu, and congruent melting point, respectively. Besides, their results showed that by decreasing particle size the congruent melting point linearly shifted to the Au – rich corner of the phase diagram which contradicts the results of Guisbiers et al. Using a nano-thermodynamic model, Chernyshev [12] calculated the phase diagram of ultrasmall ($d=2$ nm, 4 nm, and 8 nm) spherical nanoparticles of Au-Cu alloy. He reported approximately 470, 400, and 400 K decrease in melting temperatures of Au, Cu, and congruent alloy, respectively, for nanoparticles with diameter of $d=4$ nm. Also, the calculated phase diagrams by Chernyshev [12] showed that the congruent melting point transfers to higher Au concentrations as the size of the particles decreases which is consistent with the results of Cui et al. [11]. However, the calculated melting temperatures of Au and Cu by Chernyshev [12] do not conform to the reported results by Cui et al. [11] Most recently, Muñoz and Rosales [13] studied the phase diagram of the Au-Cu nanoparticles with various polyhedral shapes by using a set of MD simulations. They found that there was a shift in the location of the congruent melting point towards high concentrations of Cu as the size of the system decreased, which conforms with the results reported by Guisbiers et al., nevertheless calculated melting temperatures of pure elements and congruent melting temperatures are different from those of calculated by Guisbiers et al. According to the literature, although many attempts have been made to calculate the size dependent phase diagram of the Au – Cu system, reported results are inconsistent and contradictory. Due to the lack of sufficient experimental data, the results of the calculations have not been compared with the experimental results in any of the previous studies. So, it is impossible to judge the validity of the presented results.

*Corresponding Author

Recently, Chu et al. [14] Experimentally measured the melting temperature of Au – Cu alloy nanoparticles with a composition of 50% and a particle size of 10 nm. They also used the CALPHAD (CALculation of PHase Diagrams) method to calculate the phase diagram of Au – Cu nanoparticles. Experimental results showed that the temperatures of solidus and liquidus for the studied nanoparticles are 1028.6 K and 1041.3 K, respectively. However, in this study, the effect of size on the chemical composition of the congruent alloy has not been discussed. Also, their calculations were limited to nanoparticles bigger than 10 nanometers in diameter.

CALPHAD (CALculation of PHase Diagrams) method is a reliable and powerful technique for predicting phase diagram of bulk alloys which can be extended to nano-scale systems by adding the surface Gibbs free energy contributions to the total Gibbs energy of the system [8]. In conventional nano – CALPHAD models [8,14,15], the size dependency of the surface energies is neglected and replaced by the surface energies of the bulk materials. So, it is believed that conventional nano - CALPHAD models cannot be applied to nanoparticles generally smaller than 10 nm in diameter [16]. Recently Monji and Jabbareh [17], by considering the size dependent surface energies of the nanoparticles modified the conventional nano - CALPHAD models. This modified model can be applied to nanoparticles under critical size ($d < 10$ nm). The model has been used to calculate the phase diagram of Ag – Au [17] and Ag – Cu [17,18] nanoparticles with $d < 10$ nm and the achieved results have shown good agreements with the experiments.

This work aims to reassess the phase diagram of Au– Cu nanoparticles to answer the question of how the congruent melting temperature and the concentration of the congruent alloy in the Au – Cu system are affected by reducing the particle size. Whereas previous research works have given completely opposite answers to this question. To this end, the previously developed model by the authors [17] was applied to Au–Cu nanoparticles with different sizes from 4 nm to 40 nm in diameter. The effect of particle size on the phase diagram, congruent melting point, and congruent alloy composition are calculated theoretically and discussed in this work.

2. Model

Total Gibbs free energy of a nanoparticle system could be expressed as:

$$G^{\text{nano}} = G^{\text{bulk}} + G^{\text{surf}} \quad (1)$$

where G^{bulk} and G^{surf} are the Gibbs free energy of the bulk alloy and the surface contribution to the Gibbs free energy, respectively. The molar Gibbs free energy for two component alloys in their bulk state can be described as [8]:

$$G^{\text{bulk}} = X_A G_A^0 + X_B G_B^0 + RT(X_A \ln X_A + X_B \ln X_B) + G^{\text{ex, Bulk}} \quad (2)$$

where R and T are the universal gas constant and absolute temperature, respectively. X_i ($i=A$ or B) is the molar fraction and G_i^0 is the standard Gibbs energy of component i . $G^{\text{ex, Bulk}}$ is the excess Gibbs energy of the bulk alloy. The excess Gibbs energy can be defined by the Redlich–Kister polynomials as [20]:

$$G^{\text{ex, Bulk}} = X_A X_B \sum L_v (X_A - X_B)^v \quad (v=0, 1, 2, \dots) \quad (3)$$

where L_v is the interaction parameter and can be expressed as:

$$L_v = a_v + b_v T + c_v T \ln T + \dots \quad (4)$$

where a_v , b_v , and c_v are empirical constants.

The surface contribution to the Gibbs energy for an isotropic spherical nanoparticle is defined as [15]:

$$G^{\text{surf}} = 2CV_{AB} \sigma_{AB} / r \quad (5)$$

where σ_{AB} is the surface energy of alloy nanoparticles, V_{AB} is the molar volume and r is the particle radius. The effects of shape, surface strain, and uncertainty of the surface energy measurements are also introduced as C which is known as the correction factor. The value of C for the liquid phases and spherical solid particles is considered to be unity [21].

Because the excess volume quantity is negligible in metallic binary alloys, the molar volume of the binary alloys, V_{AB} could be defined as:

$$V_{AB} = X_A V_A + X_B V_B \quad (6)$$

where V_i is the molar volume of the pure component i . The surface energy of liquid alloys could be calculated using Butler's equation [22]. In the case where the changes in shape and surface strain with the composition are negligible, Butler's model is still applicable for the calculation of the surface energy of solid alloys [8]. The Butler's equation for an A-B binary alloy is expressed as:

$$\sigma_{AB} = \sigma_A + \frac{RT}{A_A} \ln \left(\frac{X_A^{\text{surf}}}{X_A^{\text{bulk}}} \right) + \frac{1}{A_A} [G_A^{\text{ex, surf}}(T, X_B^{\text{surf}}) - G_A^{\text{ex, bulk}}(T, X_B^{\text{bulk}})] = \sigma_B + \frac{RT}{A_B} \ln \left(\frac{X_B^{\text{surf}}}{X_B^{\text{bulk}}} \right) + \frac{1}{A_B} [G_B^{\text{ex, surf}}(T, X_A^{\text{surf}}) - G_B^{\text{ex, bulk}}(T, X_A^{\text{bulk}})] \quad (7)$$

where σ_i is the surface energy of the element i . A_i , is the molar surface area of element i when a close-packed monolayer is assumed. X_i^{surf} and X_i^{bulk} are concentrations of component i , respectively, in the surface and bulk phases. $G_i^{\text{ex, surf}}$ and $G_i^{\text{ex, bulk}}$ also indicate the partial excess Gibbs energy of component i in surface and the bulk phases.

The molar surface area of the component i could be calculated from Eq. (8) as follows:

$$A_i = 1.091 N_0^{1/3} (V_i)^{2/3} \quad (8)$$

where N_0 is Avogadro's number. $G_i^{\text{ex, surf}}$ could be expressed as [15]:

$$G_i^{\text{ex, surf}}(T, X_j^{\text{surf}}) = \alpha G_i^{\text{ex, Bulk}}(T, X_j^{\text{Bulk}}) \quad (9)$$

where α resembles the ratio of the coordination number in the surface to that in the bulk. The values of α in the liquid and solid phases were estimated to be equal to 0.85 and 0.84, respectively [15].

It should be mentioned that in conventional nano – CALPHAD models, the surface energy of the pure components, σ_i , is replaced by the surface energy of the pure elements in the bulk state. In this model, however, we apply the size dependent surface energy adopted by Xiong et al. [23] to calculate the value of σ_i as follows:

$$\sigma_i = \sigma_i^\circ (1 - 1.45 h_i/d) \quad (10)$$

where σ_i° is the temperature dependent surface energy of the element i at the bulk state, h_i is the atomic diameter of element i , and d is the particle diameter.

In the present study, the above model is used to calculate the phase diagram of spherical Au-Cu alloy nanoparticles and the outcomes are compared with available empirical and theoretical results. The information of thermodynamic and physical properties used in the present study are listed in Table 1. The values of the standard Gibbs energies, G_i° , are taken from the SGTE database for pure elements [24]. To calculate phase diagrams, above equations were implemented in a computer program which is written using Wolfram Mathematica software.

Table 1. Thermodynamic and physical properties used in the calculation of Au–Cu nanoparticle phase diagram. L denotes liquid and S denotes solid phases.

Variables	Equations	Ref.
Surface energy (J/m ²)	$L\sigma_{Au}^\circ = 1.33 - 1.4 \times 10^{-4} T$	[15]
	$S\sigma_{Au}^\circ = 1.947 - 4.3 \times 10^{-4} T$	[15]
	$L\sigma_{Cu}^\circ = 1.624 - 2.26 \times 10^{-4} T$	[25]
	$S\sigma_{Cu}^\circ = 1.953 - 2.26 \times 10^{-4} T$	[25]
Molar volume (m ³ /mol)	$L V_{Au} = 1.02582 \times 10^{-5} + 7.797 \times 10^{-10} T$	[15]
	$S V_{Au} = 1.07109 \times 10^{-5}$	[15]
	$L V_{Cu} = 6.95 \times 10^{-6} + 8.08 \times 10^{-10} T$	[25]
	$S V_{Cu} = 7.09 \times 10^{-6}$	[25]
Excess Gibbs energy (J/mol)	$L G_{Au,Cu}^{Ex,Bulk} = X_{Au} X_{Cu} [(-28230 + 3 T)]$	[26]
	$+ X_{Au} X_{Cu} [(3200 + 2 T)(X_{Au} - X_{Cu})]$	
	$+ X_{Au} X_{Cu} [(3900 - 5 T)(X_{Au} - X_{Cu})^2]$	
	$S G_{Au,Cu}^{Ex,Bulk} = X_{Au} X_{Cu} [(-28000 + 7.8.8 T - 10 T \ln T)]$	[26]
	$+ X_{Au} X_{Cu} [(6000)(X_{Au} - X_{Cu})]$	
Atomic diameter (nm)	$h_{Au} = 0.27$	[27]
	$h_{Cu} = 0.27$	[27]

3. Results and discussion

Figure 1 shows the calculated surface energy of the liquid and solid Au – Cu nanoparticles with $d=10$ nm and $d=4$ nm as a function of Au composition. Calculated surface energy at the bulk state ($d=\infty$) is also plotted for comparison. As shown in figure 1 in all cases, surface energy decreases nonlinearly along with increasing Au concentration. According to Table 1, the gold surface energy is smaller than copper's for both liquid and solid states. So, it is reasonable that increasing Au content reduces the surface energy of the system. The non-linear dependency of surface energy to Au concentration also indicates that Au tends to segregate on the surface. These findings agree well with the results reported in Ref. [28]. The results also represent that decreasing the particle size decreases the surface energy of the nanoparticle which is in accordance with the previous reports on the surface energy of alloy nanoparticles [28,29]. The variation of surface energy between the bulk and the nanoparticles leads to the difference in calculated values of the surface contribution of the Gibbs free energy. However, in some previous thermodynamic models for calculation of Au – Cu nano-phase diagrams [10] the differences between the bulk and the nanoparticles surface energy were ignored.

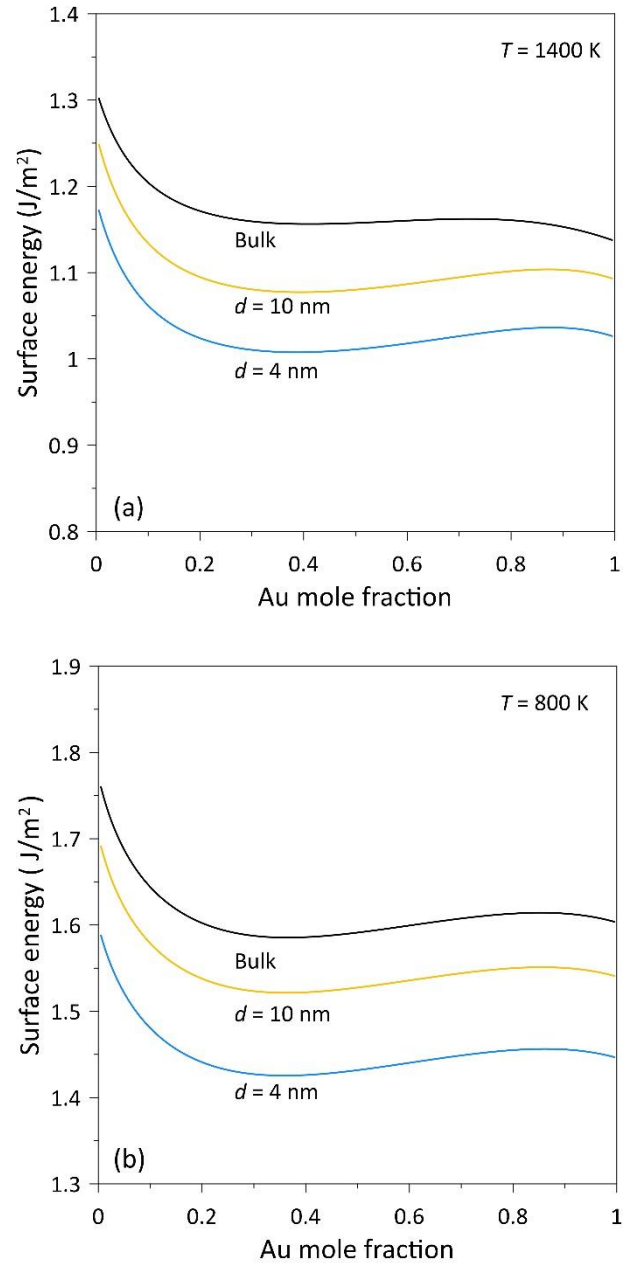


Figure 1. Calculated surface energy of Au – Cu nanoparticles with different diameters in comparison with the bulk surface energy. (a) Liquid phase at $T=1400$ K. (b) Solid phase at $T=800$ K.

Figure 2 shows the calculated surface contribution of the Gibbs free energy, G^{surf} , for the liquid and solid Au – Cu nanoparticles in different sizes. Calculations were performed with (solid lines) and without (dashed lines) considering size effect on the surface energy of the nanoparticles. It could be found from Figure 2 that decreasing particle size increases the surface contribution of the Gibbs free energy. This is consistent with experimental observations of melting temperature depression of alloy nanoparticles with size reduction [27, 28].

It is also revealed that by considering the size effect on the surface energy, calculated values of G^{surf} become smaller than those of calculated with the surface energy of the bulk state. Although this issue is not a considerable concern for large nanoparticles, the differences between calculated values of G^{surf} , with and without considering size effect on surface energy, become significant by decreasing the particle size. It should be noted that the decrease in melting temperature of nanoparticles is directly dependent to the

increase of the surface contribution of the Gibbs energy. Therefore, it can be concluded that ignoring the size effect on surface energy leads to smaller calculated melting temperatures. According to Figure 2, it is clear that the particle size decrement leads to noticeable difference in calculated melting temperatures (solidus and liquidus temperatures) between conventional and modified nano – CALPHAD models.

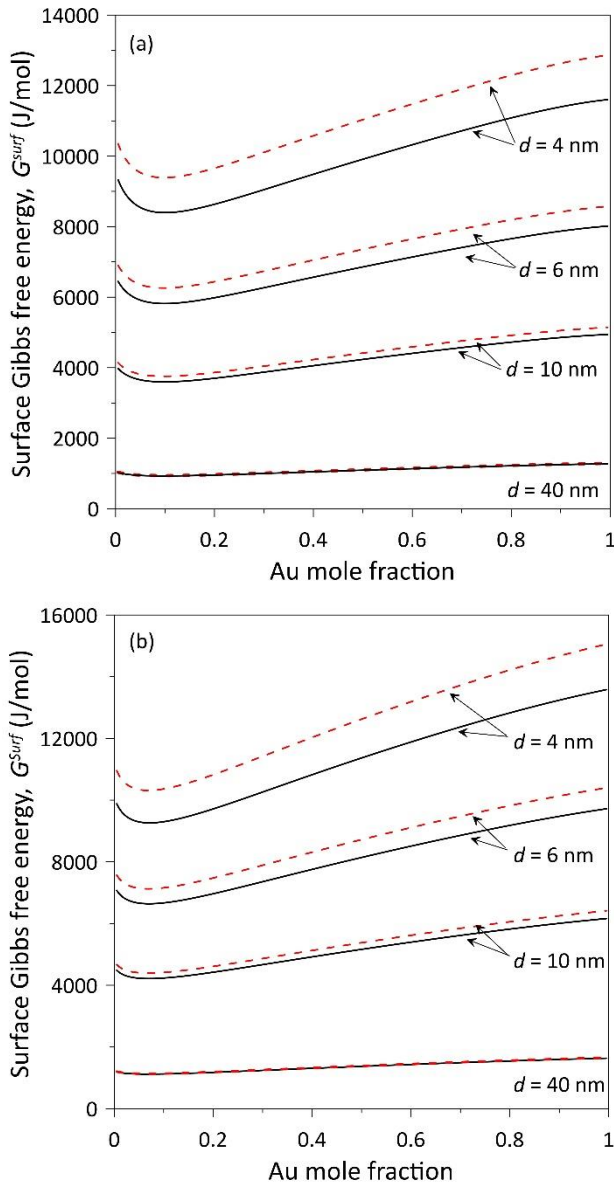


Figure 2. Calculated surface contribution of the Gibbs free energy for nanoparticles with $d= 4, 6, 10$ and 40 nm. Solid lines denote the calculations with considering size effect on the surface energy, and dashed lines indicates calculations with the surface energy of the bulk. (a) Liquid phase at $T=1400$ K. (b) Solid phase at $T=800$ K. (Figure is in color in the on-line version of the paper).

Calculated phase diagram of Au–Cu nanoparticles with $d=20$ nm, $d=10$ nm, and $d=4$ nm together with the bulk Au–Cu phase diagram are presented in Figure 3. The solidus temperatures calculated by Cui et al. [11] and Chernyshev [12] for some specific compositions are also given for comparison. In addition, experimental solidus temperature

[14] for Au-50%Cu nanoparticles with a diameter of 10 nm is also plotted on the figure 3.

The results show that decreasing the particle size leads to decrements in solidus and liquidus temperatures. This observation is consistent with the previously reported data where the size effect on nano-alloys phase diagram was studied [33]. However, the solidus temperatures calculated in this work are greater than those reported by Cui et al. [11] and Chernyshev [12]. This is reasonable because, as mentioned earlier in the introduction, the effect of size on surface energy is not considered in previous works, so these models are expected to predict smaller melting temperatures.

In addition, the calculated solidus temperature for nanoparticles with a diameter of 10 nm is greater than those achieved from experiments [14]. When comparing the experimental results with those achieved from computations, it should be noted that the experimental results are actually related to a set of nanoparticles with a size distribution of 7 to 14 nanometers [14], so, a difference in results between experimental data and those of modeling is expected. In addition, it should be brought to attention that the CALPHAD method is a semi-empirical technique, and the use of appropriate experimental data is essential to be able to optimize the model parameters and computational accuracy. The use of appropriate experimental data to determine the surface energy functions of solid and liquid phases as well as the molar volume functions is also a determining factor in accuracy of calculations. However, the experimental data of these parameters are rarely available in case of nano-alloys.

According to the phase diagrams calculated for 20, 10, and 4 nm nanoparticles, as the particle size reduces the temperature drop becomes greater.

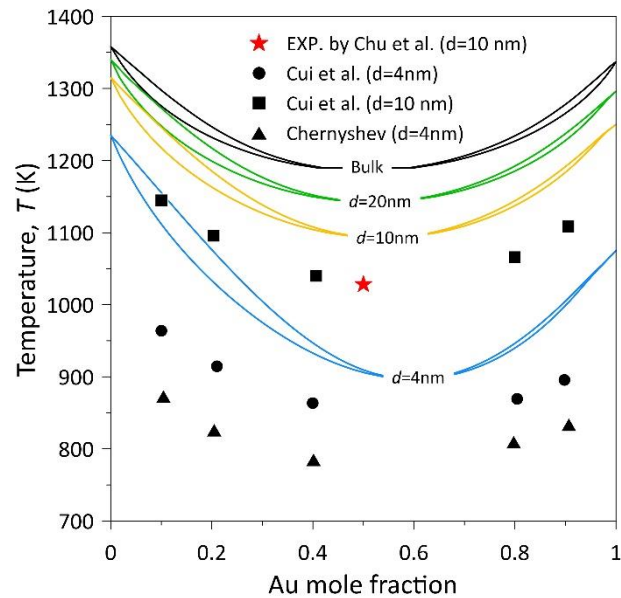


Figure 3. Calculated phase diagram of spherical Au – Cu nanoparticles with different particle sizes in comparison with the phase diagram of corresponding bulk alloy. Symbols denote calculated (Cui et al.[11] and Chernyshev [12]) or experimental (Chu et al.[14]) solidus temperatures from the literature). (Figure is in color in the on-line version of the paper).

The results also reveal that by decreasing the particle size the coexistence solid - liquid region at the Cu – rich side of

the phase diagram gets enlarged, while at the Au – rich side of the Cu-Au phase diagram the coexistence region contracts. This is due to the asymmetry of the surface contribution of the Gibbs free energy with changes in composition. As shown in Figure 2, at a certain particle size, increasing the Au concentration increases the surface Gibbs free energy. As a result, the relative position of the Gibbs free energies of the solid and liquid phases changes in comparison to the bulk. Therefore, changes in coexistence regions are expected. These findings are in contradiction with those reported in the literature. Cui et al. and Chernyshev predicted that decreasing the particle size slightly reduced the coexistence region size in the Cu – rich side of the phase diagram while considerable contraction of the coexistence region at the Au side were observed. Guisbiers et al. [10] reported that decreasing the particle diameter expanded the coexistence region at the Au – rich side of the phase diagram and contracted the coexistence region at the Cu – rich side which is completely in contrast to our findings.

It could be understood from figure 3 that the congruent melting point drops by decreasing the particle size and extends to the Au – rich side of the phase diagram. These findings are in agreement with the results reported by Cui et al. [11] and Chernyshev [12]. In contrast, Muñoz and Rosales [13] and Guisbiers et al. [10] predicted a shift in the congruent melting point towards high concentrations of Cu. Muñoz and Rosales and Guisbiers et al. also reported that for nanoparticles with $d = 4$ nm, the melting temperature of copper is lower than that of gold unlike the bulk state, which contradicts our findings and the results reported by Cui et al. and Chernyshev.

Unfortunately, there is not sufficient empirical data in the literature on the phase diagram of Au –Cu alloy nanoparticles. Hence, to investigate the validity of our results the calculated melting temperature of pure Au and Cu have been compared to the experimental [27,30,31] and MD simulation results [36] reported by others. Figure 4 (a) shows the calculated melting temperature of Au nanoparticles in this work in comparison with experimental data reported by Buffat and Borel [34]. Calculated melting temperatures by Vallee et al. [9], Cui et al. [11], and Chernyshev [12] are also plotted for comparison. As can be seen, calculated melting temperatures in this work are in good agreement with the experimental data. Especially in case of very small nanoparticles (e.g., $d=4$ nm) our results show better agreements with experiments than the outcomes of Vallee et al., Cui et al., and Chernyshev. In Figure 4 (b), the calculated melting temperature of Cu nanoparticles has been compared with experimental data reported by Huang et al. [31] and Cui et al. [35] and MD simulation results performed by Delogu [36]. It is readily apparent that calculated melting temperatures of Cu in this work show excellent agreement with experimental and MD simulation results. It is also clear that the predicted melting temperatures by Cui et al. and Chernyshev are very smaller than either the experimental or calculated temperatures in this work. It is also found from figures 3(a) and 3(b) that at any given particle diameter, the melting temperature of Cu nanoparticles is higher than that of their Au counterpart. Thus, in calculations of Muñoz and Rosales [13] and Guisbiers et al. [10] where the melting temperature of Cu nanoparticles were predicted to be lower than the melting temperature of their Au counterparts by size decrement, cannot be confirmed.

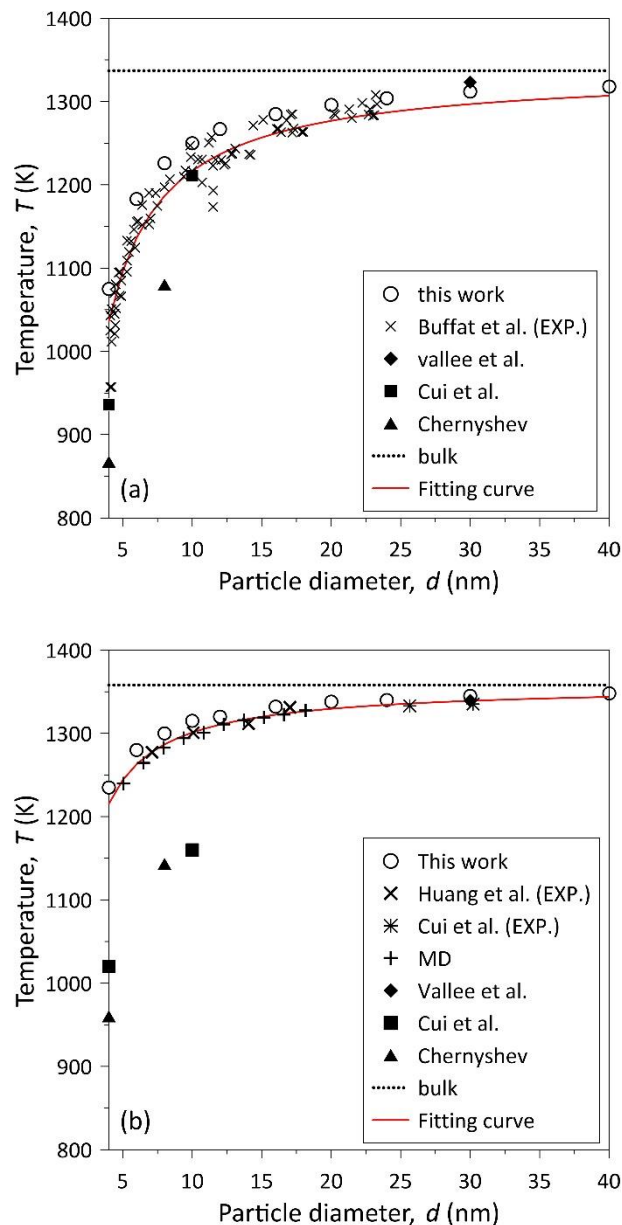


Figure 4. Calculated melting temperature of (a) Au and (b) Cu nanoparticles in this work together with calculated temperatures by Vallee et al. [9], Cui et al. [11], and Chernyshev [12] as well as some experimental data [27,30,31] and MD simulation results [36]. Solid lines indicate fitting curves for experimental data. (Figure is in color in the on-line version of the paper).

It is well known that the melting temperature of a nanoparticle can be derived by Eq.(11) [37]:

$$T_{m,NP}=T_{m,b}(1-\beta/d) \quad (11)$$

where $T_{m,NP}$ and $T_{m,b}$ are the nanoparticle and bulk melting temperatures, respectively, d is the particle diameter and β is material constant. Eq. (11) can be applied to other transition temperatures as well [38]. We applied this model to predict the congruent melting temperature in Au – Cu system. To this end, Eq. (11) fitted to the experimental data on melting temperatures of Au and Cu (solid lines in Figures 3(a) and 3(b)) and the material constant, β , were derived as 0.9 nm and 0.42 nm for Au and Cu, respectively. Then, we estimated β for binary alloy system as $\beta_{Au-Cu}=X_{Au}\beta_{Au}+X_{Cu}\beta_{Cu}$ where X_i is the mole fraction of i component. Since at congruent melting temperature of the bulk alloy $X_{Au}\approx X_{Cu}\approx 0.5$, the value

of $\beta_{\text{Au}-\text{Cu}}$ is calculated as 0.66 nm. According to the calculated phase diagram of the bulk alloy, the congruent melting temperature is 1190 K; Therefore, size dependent congruent melting temperature of Au–Cu alloy can be estimated from Eq. (12):

$$T_{\text{cong},\text{NP}}=1190(1-0.66/d) \quad (12)$$

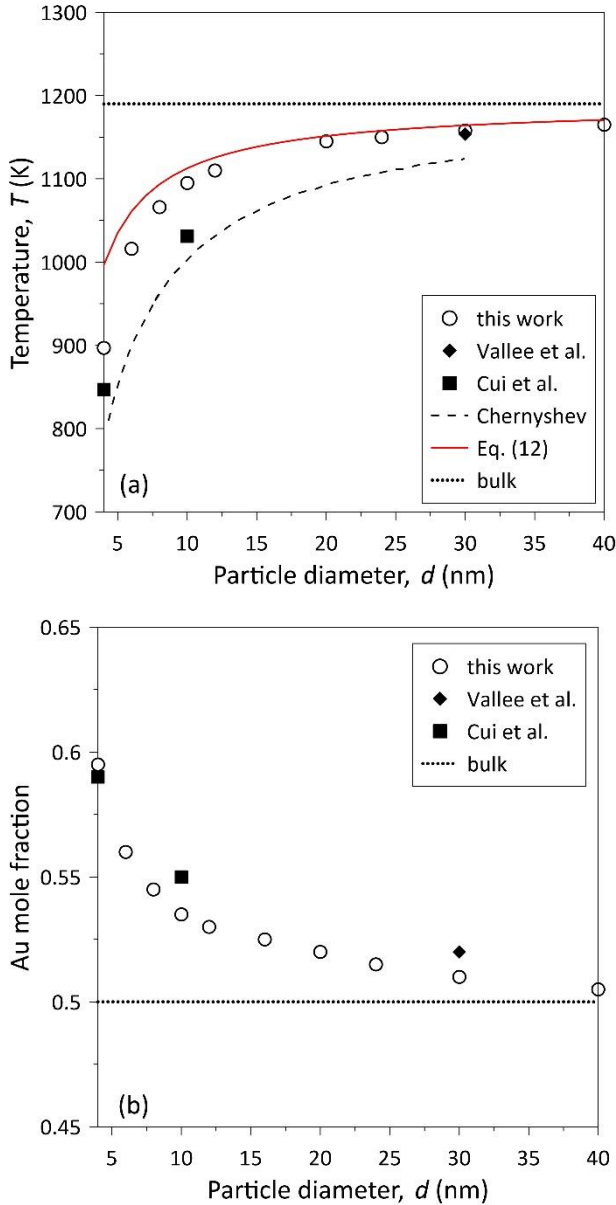


Figure 5. Calculated congruent melting point (a) and congruent alloy composition (b) as a function of particle diameter in comparison with previous calculations (Vallee et al. [9], Cui et al. [11], and Chernyshev [12]). (Figure is in color in the on-line version of the paper).

Figure 5(a) shows the congruent melting temperature of Au – Cu nanoparticles calculated from Eq (12) (solid line) together with calculated results of the thermodynamic model and those reported by Vallee et al., Cui et al. and Chernyshev. Depression of the congruent melting temperature by decreasing the particle size is evident. Also, calculated values of T_{cong} from Eq. (12) and the thermodynamic model in this work are in good agreement. It should be noted out that it is assumed that the composition of the congruent alloy is constant for all particle diameters in the development of Eq. (12). This assumption leads to a size

independent material constant, β . However, calculated results in this work (Figure. 4(b)) and those reported in the literature [10–13] show that the congruent alloy composition is size dependent. So, a discrepancy between the achieved results by the analytical model (Eq. (12)) and those calculated by using the CALPHAD approach is expected. It is also noteworthy that by increasing the particle size, this difference becomes negligible.

Variations of congruent alloy composition with respect to the particle diameter are shown in Figure 5(b). As can be seen, decreasing the particle size increases the Au content of the congruent alloy composition which is consistent with the results reported by Cui et al. and Chernyshev. However, in contrast to Cui et al., our results show non – linear dependency of congruent alloy composition to the particle size.

4. Conclusion

Size dependent phase diagram of Au – Cu nano-alloy was recalculated based on a CALPHAD type thermodynamic model. The results showed that decreasing the particle size leads to a drop in solidus, liquidus, and congruent melting temperatures. It was also found that by decreasing the particle size the coexistence solid – liquid phase region contracts at the Au – rich side of the phase diagram while it was expanded at the Cu – rich side of the phase diagram. The results cleared that by reducing the particle size the composition of congruent alloy extends to the Au – rich side of the phase diagram. In comparison with previous calculations, calculated results in this work showed better agreements with experiments. The results can be used as a guideline for the design of Au – Cu bimetallic nano-catalysts.

Nomenclature

A_i ($i = A, B$)	: molar surface area of pure elements (m^2/mol)
a_v, b_v, c_v	: empirical constants (J/mol)
C	: correction factor
d	: particle diameter (m)
G^{nano}	: total Gibbs free energy at nanoscale (J/mol)
G^{bulk}	: Gibbs free energy of bulk state (J/mol)
G^{surf}	: surface contribution to the Gibbs free energy (J/mol)
G_i^0 ($i = A, B$)	: standard Gibbs energy of pure elements (J/mol)
$G^{\text{ex,Bulk}}$: excess Gibbs energy of bulk state (J/mol)
$G_i^{\text{ex,surf}}$ ($i = A, B$)	: excess Gibbs energy of pure elements in surface (J/mol)
$G_i^{\text{ex,bulk}}$ ($i = A, B$)	: excess Gibbs energy of pure elements in bulk phase (J/mol)
h_i ($i = A, B$)	: atomic diameter (m)
L_v	: interaction parameter (J/mol)
N_0	: Avogadro's number
R	: universal gas constant ($\text{J}/\text{mol.K}$)
r	: particle radius (m)
T	: absolute temperature (K)
V_i ($i = A, B$)	: molar volume of pure elements (m^3/mol)
V_{AB}	: molar volume of nanoparticles (m^3/mol)
X_i ($i = A, B$)	: molar fraction of pure elements
X_i^{surf} ($i = A, B$)	: molar fraction of pure elements in surface

X_i^{bulk} ($i = A, B$)	: molar fraction of pure elements in bulk phase
α	: ratio of the coordination number in the surface to that in the bulk
σ_{AB}	: surface energy of nanoparticles (J/m^2)
σ_i ($i = A, B$)	: size dependent surface energy of pure elements (J/m^2)
σ_i^∞	: surface energy of pure elements at the bulk state (J/m^2)

References

- [1] X. Liu, A. Wang, T. Zhang, D. S. Su, and C. Y. Mou, "Au-Cu alloy nanoparticles supported on silica gel as catalyst for CO oxidation: Effects of Au/Cu ratios," *Catal. Today*, *160*, 103–108, 2011.
- [2] M. K. Birhanu *et al.*, "Electrocatalytic reduction of carbon dioxide on gold-copper bimetallic nanoparticles: Effects of surface composition on selectivity," *Electrochim. Acta*, *356*, 136756, 2020.
- [3] W. Li, A. Wang, X. Liu, and T. Zhang, "Silica-supported Au-Cu alloy nanoparticles as an efficient catalyst for selective oxidation of alcohols," *Appl. Catal. A Gen.*, *433–434*, 146–151, 2012.
- [4] M. Hajfathalian *et al.*, "Photocatalytic Enhancements to the Reduction of 4-Nitrophenol by Resonantly Excited Triangular Gold-Copper Nanostructures," *J. Phys. Chem. C*, *119*, 17308–17315, 2015.
- [5] R. Biswas, S. Singh, I. Ahmed, R. A. Patil, Y. R. Ma, and K. K. Haldar, "Rational Design of Bimetallic Au/Cu Nanostructure: An Efficient Catalyst for Methanol Oxidation," *ChemNanoMat*, *7*, 158–164, 2021.
- [6] H. M. Lu and X. K. Meng, "Theoretical model to calculate catalytic activation energies of platinum nanoparticles of different sizes and shapes," *J. Phys. Chem. C*, *114*, 1534–1538, 2010.
- [7] N. Zhao, Y. Q. He, and C. C. Yang, "A new approach to construct bulk and size-dependent continuous binary solution phase diagrams of alloys," *RSC Adv.*, *5*, 96323–96327, 2015.
- [8] T. Tanaka and S. Hara, "Thermodynamic evaluation of binary phase diagrams of small particle systems," *zeitschrift fur Met.*, *92*, 467–472, 2001.
- [9] R. Vallée, M. Wautelet, J. P. Dauchot, and M. Hecq, "Size and segregation effects on the phase diagrams of nanoparticles of binary systems," *Nanotechnology*, *12*, 68–74, 2001.
- [10] G. Guisbiers, S. Mejia-Rosales, S. Khanal, F. Ruiz-Zepeda, R. L. Whetten, and M. José-Yacaman, "Gold-copper nano-alloy, " tumbaga ", in the era of nano: Phase diagram and segregation," *Nano Lett.*, *14*, 6718–6726, 2014.
- [11] M. Cui, H. Lu, H. Jiang, Z. Cao, and X. Meng, "Phase Diagram of Continuous Binary Nanoalloys: Size, Shape, and Segregation Effects," *Sci. Rep.*, *7*, 1–10, 2017.
- [12] A. P. Chernyshev, "The influence of the size effect on the transition of Au-Cu alloy nanoparticles to the dynamic amorphous state," *Mater. Today Proc.*, *25*, 370–372, 2020.
- [13] H. R. Martínez-Muñoz and S. Mejía-Rosales, "The AuCu Phase Diagram at the Nano Scale: A Molecular Dynamics Approach," *J. Clust. Sci.*, doi: <https://doi.org/10.1007/s10876-021-02015-6>
- [14] M. Z. Chu *et al.*, "Melting and phase diagram of Au-Cu alloy at nanoscale," *J. Alloys Compd.*, *891*, 162029, 2021.
- [15] J. Park and J. Lee, "Phase diagram reassessment of Ag–Au system including size effect," *Calphad*, *32*, 135–141, Mar. 2008.
- [16] G. Garzel, J. Janczak-rusch, and L. Zabdyr, "Reassessment of the Ag – Cu phase diagram for nanosystems including particle size and shape effect," *CALPHAD Comput. Coupling Phase Diagrams Thermochem.*, *36*, 52–56, 2012.
- [17] F. Monji and M. A. Jabbareh, "Thermodynamic model for prediction of binary alloy nanoparticle phase diagram including size dependent surface tension effect," *Calphad Comput. Coupling Phase Diagrams Thermochem.*, *58*, 1–5, 2017.
- [18] M. A. Jabbareh and F. Monji, "Thermodynamic modeling of Ag – Cu nanoalloy phase diagram," *Calphad*, *60*, 208–213, 2018.
- [19] M. Z. Chu *et al.*, "Thermodynamic reassessment of the Ag–Cu phase diagram at nano-scale," *Calphad*, *72*, 102233, 2021.
- [20] N. Sunders and A. P. Miodownik, *CALPHAD (Calculation of Phase Diagrams): A Comprehensive Guide*. Pergamon, 1998.
- [21] W. H. Qi, M. P. Wang, and Q. H. Liu, "Shape factor of nonspherical nanoparticles," *J. Mater. Sci.*, *40*, 2737–2739, 2005.
- [22] J. A. V Butler, "The thermodynamics of the surfaces of solutions," *Proc. R. Soc. A*, *135*, 348–375, 1932.
- [23] S. Xiong, W. Qi, Y. Cheng, B. Huang, M. Wang, and Y. Li, "Modeling size effects on the surface free energy of metallic nanoparticles and nanocavities," *Phys. Chem. Chem. Phys.*, *13*, 10648–10651, 2011.
- [24] A. Delsante, "SGTE data for pure elements" *Calphad*, *15*, 317–425, 1991.
- [25] J. Sopousek *et al.*, "Cu – Ni nanoalloy phase diagram – Prediction and experiment," *CALPHAD Comput. Coupling Phase Diagrams Thermochem.*, *45*, 33–39, 2014.
- [26] B. Sundman, S. G. Fries, and W. A. Oates, "A thermodynamic assessment of the Au-Cu system," *Calphad*, *22*, 335–354, 1988.
- [27] K. K. Nanda, S. N. Sahu, and S. N. Behera, "Liquid-drop model for the size-dependent melting of low-dimensional systems," *Phys. Rev. A*, *66*, 013208, 2002.
- [28] J. M. McDavid and S. C. Fain, "Segregation at CuAu alloy surfaces," *Surf. Sci.*, *52*, 161–173, 1975.
- [29] F. M. Takrori and A. H. Ayyad, "Surface energy of metal alloy nanoparticles," *Appl. Surf. Sci.*, *401*, 65–68, 2017.

- [30] M. A. Jabbareh, "Size, shape and temperature dependent surface energy of binary alloy nanoparticles," *Appl. Surf. Sci.*, *426*, 1094–1099, 2017.
- [31] C.-H. Huang, H. P. Wang, J.-E. Chang, and E. M. Eyring, "Synthesis of nanosize-controllable copper and its alloys in carbon shells," *Chem. Commun.*, *2*, 4663–4465, 2009.
- [32] S. Delsante *et al.*, "Synthesis and thermodynamics of Ag–Cu nanoparticles," *Phys. Chem. Chem. Phys.*, *17*, 28387–28393, 2015.
- [33] G. Guisbiers, "Advances in thermodynamic modelling of nanoparticles," *Adv. Phys. X*, *4*, 1668299, 2019.
- [34] P. Buffat and J. P. Borel, "Size effect on the melting temperature of gold particles," *Phys. Rev. A*, *13*, 2287–2298, 1976.
- [35] Z. Cui, B. Ji, Q. Fu, H. Duan, Y. Xue, and Z. Li, "Research on size dependent integral melting thermodynamic properties of Cu nanoparticles," *J. Chem. Thermodyn.*, *149*, 106148, 2020.
- [36] F. Delogu, "Structural and energetic properties of unsupported Cu nanoparticles from room temperature to the melting point: Molecular dynamics simulations," *Phys. Rev. B - Condens. Matter Mater. Phys.*, *72*, 205418, 2005.
- [37] G. Guisbiers, "Review on the analytical models describing melting at the nanoscale," *J. Nanosci. Lett.*, *2*, 8–18, 2012.
- [38] S. S. Kim, "Thermodynamic modeling of the CeO₂ – CoO nano-phase diagram," *J. Alloys Compd.*, *588*, 697–704, 2014.